Design considerations and validation of the MSTAR absolute metrology system

Robert D. Peters*, Oliver P. Lay, Serge Dubovitsky, Johan Burger, Muthu Jeganathan
Jet Propulsion Laboratory, California Institute of Technology, 4800 Oak Grove Drive, Pasadena CA 91109

ABSTRACT

Absolute metrology measures the actual distance between two optical fiducials. A number of methods have been employed, including pulsed time-of-flight, intensity-modulated optical beam, and two-color interferometry. The rms accuracy is currently limited to ~5 microns. Resolving the integer number of wavelengths requires a 1-sigma range accuracy of ~0.1 microns. Closing this gap has a large pay-off: the range (length measurement) accuracy can be increased substantially using the unambiguous optical phase.

The MSTAR sensor (Modulation Sideband Technology for Absolute Ranging) is a new system for measuring absolute distance, capable of resolving the integer cycle ambiguity of standard interferometers, and making it possible to measure distance with sub-nanometer accuracy. In this paper, we present recent experiments that use dispersed white light interferometry to independently validate the zero-point of the system. We also describe progress towards reducing the size of optics, and stabilizing the laser wavelength for operation over larger target ranges.

MSTAR is a general-purpose tool for conveniently measuring length with much greater accuracy than was previously possible, and has a wide range of possible applications.

Keywords: Absolute metrology, distance measurement

1. INTRODUCTION

High-precision non-contact measurements of distance are required in many areas of science and engineering. In addition to well-established uses of distance metrology in optical figure sensing, high-precision metrology is also used in the semiconductor industry for lithography, mask/wafer inspection, and
for general precision-positioning applications, such as measurement and calibration of high-resolution motions and in high-precision machining.

In addition, astronomical telescopes and instrumentation depend increasingly on the use of laser metrology systems to monitor changes in the dimensions of the system at the sub-micron level. Interferometers in particular employ a number of metrology gauges to monitor beam path lengths within the instrument ('constant term' metrology), the positions of delay lines, and the lengths of baselines. Typical disturbances include high-frequency vibration, slow thermal drifts, and, for the case of ground-based instruments, changes in the refractive index of air. The metrology gauges must operate over distances ranging from a few centimeters to hundreds of meters, with nanometer or even sub-nanometer precision. Systems in use are almost invariably differential in nature, able to measures changes in length, but not the absolute length itself. Although well-suited to measuring high-frequency fluctuations, measurements over longer timescales require uninterrupted operation and must be calibrated to a starting point or 'home' position. Breaking the beam causes the fringe count to be lost, and the calibration must be repeated. In a number of situations, measuring a baseline length for example, a differential gauge is simply insufficient. What is needed is an absolute metrology gauge that can operate over large distances with nanometer precision, and that is robust to interruptions of the beam.

Standard laser interferometry is an established method for displacement measurement; sub-nanometer precision has been achieved[1,2], but absolute distance is ambiguous, because of the inherent half-wavelength (~0.5 μm for a near-IR laser) ambiguity range. This is known as the 'integer cycle ambiguity'. To determine the target distance with high accuracy, the

ambiguity range of the fine interferometric stage must be resolved with an additional coarse gauge(s). The range accuracy of the coarse stage must be better than the ambiguity range of the fine stage; resolving a half-wavelength ambiguity range of 0.5 μm requires a 1σ absolute range accuracy of ~0.1 μm (peak-valley error ~0.5 μm), significantly beyond the existing capability.

A number of methods exist for the unambiguous measurement of target distance. The most common method, based on the time-of-flight[3] of emitted pulses, cannot achieve the necessary accuracy, because a timing accuracy of 0.6 femtoseconds is required for a range accuracy of 0.1 μm. Other techniques, such as intensity-modulated optical beam[4,5], frequency-modulated optical beam, and two-color interferometry[6] are used where higher accuracy is required. The rms accuracy is currently limited to ~5 μm, although there are examples of higher accuracy in more restricted applications, usually at very short target distances[7-10]. The methods relying on the generation and detection of high-frequency optical carrier modulation suffer from the low responsivity of the high-speed photodetectors required for their operation, and the need for high-speed signal processing electronics.

Two-color interferometry is the most promising approach, in which two laser interferometer measurements are made at different laser wavelengths. Differencing these measurements is equivalent to having a laser interferometer with a much longer synthetic wavelength[6]. High accuracy over large distances imposes four requirements: (1) the coherence length of the laser must be longer than the round-trip distance to be measured; (2) the laser wavelength must be known to the accuracy needed for the measurement (10 nm accuracy at 100 m requires 10^{-10} wavelength knowledge); (3) the combination of synthetic wavelength and phase resolution must be sufficient to achieve the 0.1 μm accuracy; and (4) the synthetic wavelength must be known with high accuracy (0.1 ppm for 1 m distance, 0.01 ppm for 10 m distance, etc.). This combination has not been achieved with existing lasers.

In this paper we discuss a new architecture that overcomes the existing limitations, and experimentally demonstrate unambiguous measurements with resolution sufficient to resolve the integer cycle ambiguity. The technique, Modulation Sideband Technology for Absolute Ranging (MSTAR), implements a two-color metrology system using a single narrow-linewidth, frequency-stabilized laser; the multiple wavelengths are produced as phase modulation sidebands using fast integrated-optics modulators. This two-color approach avoids the need for the fast photodetectors and signal processing required for other RF modulation schemes[4,5], and the fine and coarse stages are seamlessly integrated into a single high accuracy absolute sensor.

The next section describes the principle of operation and how the MSTAR system has been implemented in the lab. Section 3 describes results from the experiments used to validate the performance of the sensor, and Section 4 discusses how MSTAR is easily extended to operate over long distances and how the beam launcher optics can be miniaturized into compact and robust package.

2. THE MSTAR SYSTEM

2.1. Principle of operation

The system is shown in Fig. 1. The laser light, frequency ν, is split into the Measurement and Local arms. In the Measurement arm; the laser frequency is up-shifted by f_M, and a sinusoidal phase modulation $\Delta\Phi \sin(2\pi F_M t)$ is applied, producing a series of sidebands spaced by $\pm F_M$, $\pm 2F_M$, $\pm 3F_M$, ..., with amplitudes given by Bessel functions. Similar modulation, using slightly different frequencies, is applied to the Local arm. The resulting optical spectrum for the Measurement and Local beams is shown in Figure 1b (higher order sidebands have been omitted for clarity). The upper and lower sidebands correspond to the two wavelengths of a two-color interferometer. The Measurement and Local beams mix at the detectors, generating the down-converted frequencies shown in Figure 1c (note that MSTAR does not require high speed photodetectors). These photodetector outputs are bandpass filtered to isolate the sinusoids for the carrier, upper, and lower sidebands.

* robert.d.peters@jpl.nasa.gov; phone 1 818 393-6263; fax 1 818 393-9471

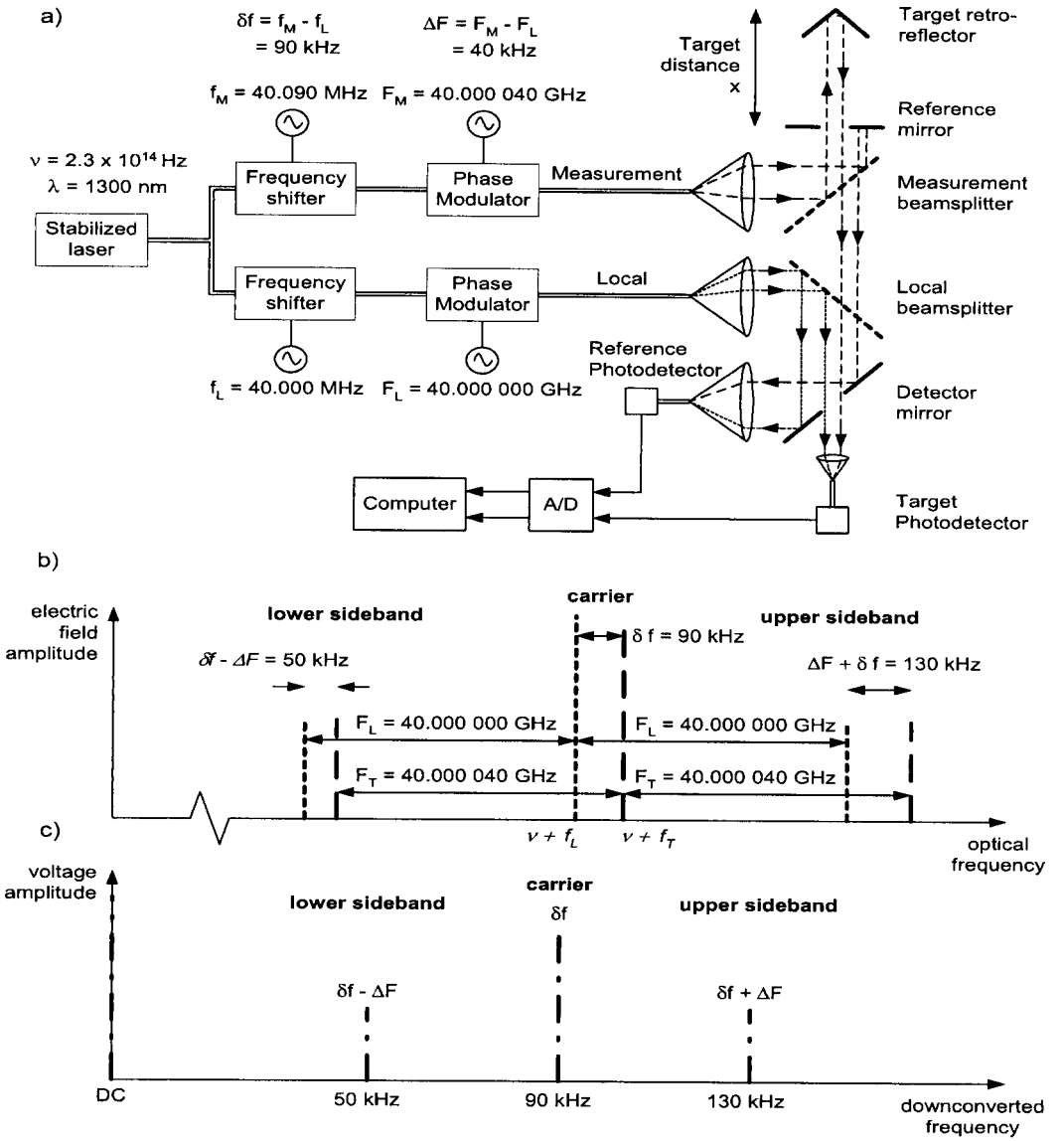

Figure 1: (a) Schematic of the *MSTAR* system. The distance to be measured, x, lies between the reference mirror and the target retro-reflector. (b) Optical spectrum before photo-detection. Long-dash = measurement beam; short-dash = local beam (c) Spectrum of electrical signals after photo-detection.

The phase difference in cycles (1 cycle=2π radians) between the carrier sinusoids from the Target and Reference detectors (each with frequency δf) is given by $\Delta\phi_{car} = (\nu + f_M)(2x/c)$ where x is the distance between the reflecting surface of the reference mirror and the vertex of the target retro-reflector, and c is the speed of light. The integer number of cycles is unknown and the resulting estimate of x is ambiguous:

$$x_{car} = \frac{c}{2(\nu + f_M)}(\Delta\phi_{car} \pm m) = L(\Delta\phi_{car} \pm m) \tag{1}$$

where m is an integer. The ambiguity length L is approximately half the laser wavelength. The 1σ-precision of the length measurement (σ_x) depends on the precision of the phase difference: $\sigma_x = L\sigma_{\Delta\phi}$. This carrier measurement is equivalent to a standard heterodyne metrology gauge.

In addition to making this sub-nanometer measurement, MSTAR uses the sidebands to determine the number of integer cycles m in Eq. 1. The upper sideband has a phase difference of $\Delta\phi_{usb} = (\nu + F_M + f_M)(2x/c)$ between Target and Reference outputs. The lower sideband gives $\Delta\phi_{lsb} = (\nu - F_M + f_M)(2x/c)$. These phase differences are combined to yield

$$x' = \frac{c}{4F_M}(\Delta\phi_{usb} - \Delta\phi_{lsb} \pm n) = L'(\Delta\phi_{usb} - \Delta\phi_{lsb} \pm n) \tag{2}$$

analogous to Eq. 1, but with a substantially longer ambiguity length, $L' = c/(4F_M)$, and precision $\sigma_x' = L'\sqrt{2}\sigma_{\Delta\phi}$. The synthetic wavelength is $c/2F_M$. As an example of how measurement of x' can be used to resolve ambiguity m consider the frequencies shown in Fig. 1. The carrier phase ambiguity length is L = 0.65 μm. With a phase resolution of $\sigma_{\Delta\phi}$ = 5 x 10^{-5} cycles (0.3 mrad), σ_x = 30 pm. The sideband combination has L' = 1.875 mm and σ_x' = 0.12 μm, sufficient to resolve L (and therefore m) at a high level of probability. The remaining ambiguity (n in Eq. 2) can be resolved by switching to a lower phase modulation frequency. Switching to a phase modulation frequency of 30 MHz gives L'' = 2.5 m and σ_x'' = 0.18 mm, sufficient to resolve n. This is illustrated schematically in Fig. 2.

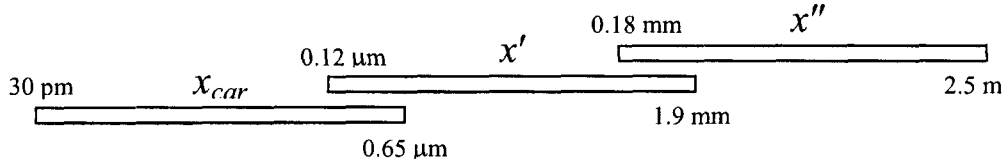

Figure 2: Schematic representation of the 3 stages of length measurement given in the text. The left end of each bar indicates the resolution of the measurement; the right end indicates the ambiguity length. Lower resolution stages are easily added.

The above analysis neglects the effects of air dispersion, phase offsets in the detectors and path imbalances within the optics. With strong phase modulation, it is also possible to use the higher order sidebands to improve performance.

2.2. Implementation

There are two key challenges to implementing MSTAR as an absolute metrology system: (1) generating the high frequency modulation sidebands; (2) achieving the required phase precision.

The system in Fig. 1 was mounted on a floating optical table in a laboratory environment. The laser is an Nd:YAG system with linewidth of 10 kHz at 1.32 μm. The wavelength is measured against a HeNe reference laser using a Burleigh WA-1500 wavemeter (accuracy ~0.1 ppm). The light is frequency shifted using acousto-optic modulators by ~40 MHz, and then fed into high-frequency phase modulators operating at ~40 GHz.

The phase modulators for the initial experiments were polymer-based integrated optics devices[9] built by USC and Pacific Wave. These are potentially more efficient at high frequencies than $LiNbO_3$ devices, due to a better velocity match between the RF and optical waves, and have a fiber-to-fiber insertion loss of ~12dB. The phase modulators are driven at ~40 GHz by a pair of Agilent 83650B synthesizers (accurate to ~0.1 ppm) and MMIC amplifiers. With +23 dBm of RF input power to the modulators, the first sidebands are 12 dB down from the carrier in the post-detection spectrum. More recent results have been obtained using commercially-available 40 GHz modulators from EOSpace which have a much lower insertion loss.

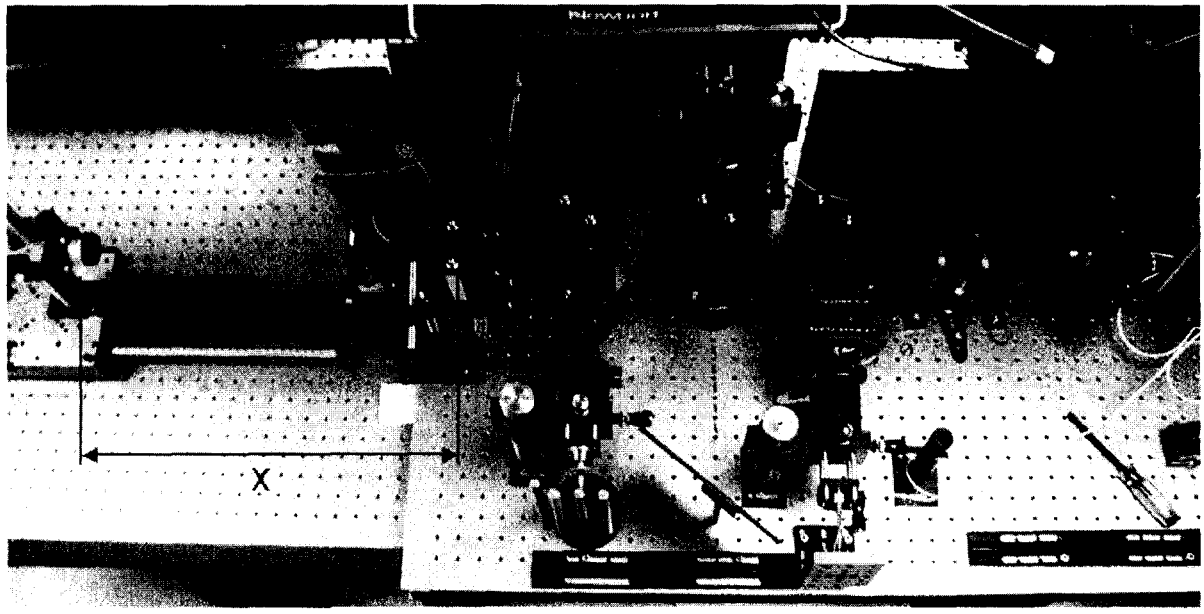

Figure 3: Photograph of the MSTAR optics in the lab. The dimension x indicates the separation of the target retro-reflector on the left and the annular MSTAR reference mirror. The Measurement collimator is at the lower center. To the right of this is the Reference collimator. The Local collimator is in the upper center, and the Target collimator is at the far right.

The Measurement and Local beams are formed by collimating the fiber outputs with 50 mm achromatic lenses. The optics were designed to minimize multi-path effects. A phase accuracy of 5 x 10^{-5} cycles requires an isolation of ~75 dB between the four alternative paths from the laser to the detectors. The dimensions of the annular mirrors were optimized, and a large effort went into minimizing leakages in the system. A set of polarizing optics (not shown in Fig. 1a) was used to increase the isolation to meet the requirement. The target retro-reflector is attached to a 1-meter manual translation slide. The photodetectors are New Focus 2011 units. The outputs are digitized at 500 kHz and processed in the computer to generate the MSTAR output. Each measurement is based on 60,000 samples (0.12 seconds).

The phase as a function of time for each component in the RF spectrum (Fig. 1c) for each detector output is obtained with the following procedure. (1) Each time series is Fourier transformed. (2) The negative frequencies are discarded. (3) For each carrier/sideband in the spectrum, a block of channels centered on the nominal line frequency is extracted. (4) This segment of the spectrum, shifted to DC, is then Fourier transformed to give a complex function in the time domain. The complex argument of this function is the phase of the sideband over the 0.13 s period, $\Delta\phi_k^{(T)}$ or $\Delta\phi_k^{(R)}$. (5) For each carrier/sideband we difference the phases obtained for the Target and Reference detectors, $\Delta\phi_k = \Delta\phi_k^{(T)} - \Delta\phi_k^{(R)}$. The process is essentially a Hilbert transform[12] of the original time series, with additional filtering and down-conversion to isolate the different spectral components, and is much more robust than a zero-crossing approach to phase measurement.

In order to verify the accuracy of MSTAR, measurements were compared with a phase meter developed for the Space Interferometry Mission (SIM)[13]. This phase meter, not shown in Fig. 1a, is connected to the outputs of the photodetectors, in parallel with MSTAR data acquisition. It first converts the heterodyne sine wave to square waves to reduce amplitude dependence, then it measures the time between the signals on the measurement and reference channel. The phase meter also counts the integer number of cycles to track displacements over large distances.

3. RESULTS

Four types of experiment were conducted to validate performance: (1) a displacement test, (2) a stability test, (3) a zero test, and (4) a zero out displacement test. Each is described below.

3.1. Displacement test

From an arbitrary starting position, x_{START}, the target was moved in small increments along the track. At each position, MSTAR generated a position, x_{MSTAR}, based only on the sideband difference phases. Equation 2 shows that this measurement depends only on the phase modulation frequency (tied to the synthesizer's frequency reference), and is independent of the laser wavelength. The 'truth' measurement depends only on the accuracy of fringe counting by the independent verification phase meter, and the wavelength of the laser light (tied to the wavelength of the HeNe reference laser). An example set of data is shown in Fig. 4, with the MSTAR distance plotted against the 'truth'. Also shown is the residual, $\sigma'_x = x_{MSTAR} - \Delta x_{TRUTH} - x_{START}$ (note that x_{START} is equated to the first value of x_{MSTAR}, so that $\sigma'_x = 0$ for the first point by definition). The standard deviation of this residual (0.12 μm) is typical of the results obtained, and demonstrates that MSTAR can measure *displacements* (as opposed to absolute position) with the accuracy necessary to resolve the number of integer cycles *m*.

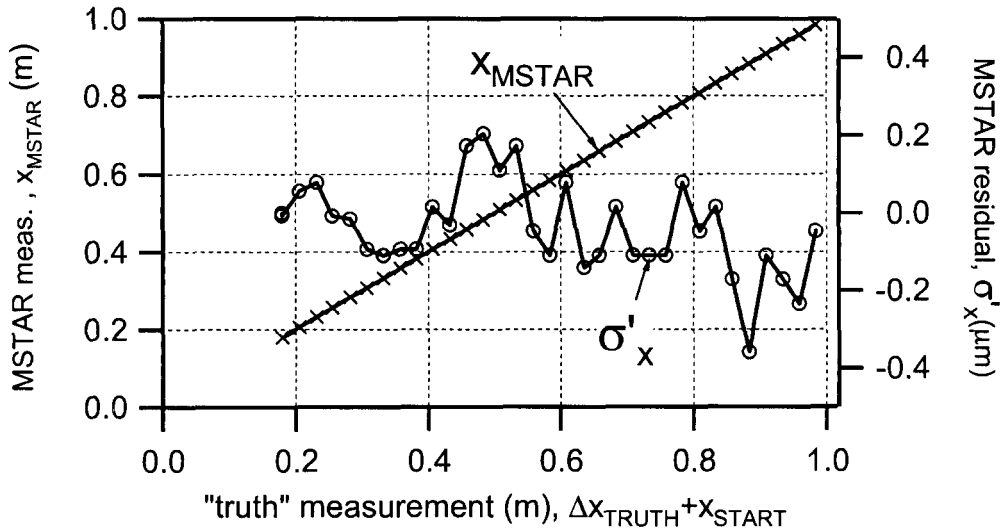

Figure 4: MSTAR absolute measurement vs 'true' displacement from start point (based on fringe counting). The residual error, $\sigma'_x = x_{MSTAR} - \Delta x_{TRUTH} - x_{START}$ is overlaid.

3.2. Stability test

This test was conducted in the same way as the displacement test, except the target was not deliberately moved (small thermal motions were tracked with the truth measurement). Over a 3-hour period, the standard deviation of the residual was 0.05 μm, demonstrating that MSTAR is stable with time.

3.3. Zero test

The displacement test described in Section 3.1 is not a complete test of an absolute metrology system, since it does not validate the zero-point of the sensor. In order to do this, the large 25-mm hollow target retro-reflector used in the two previous experiments was replaced with one 6 mm in diameter, which is small enough to fit through the central hole in the MSTAR reference mirror.

A white light Michelson interferometer was used as the independent sensor. The source was a quartz lamp, coupled into a single-mode optical fiber, and finally collimated into a parallel beam incident from the left on the MSTAR Measurement Beamsplitter (Fig. 1a). Part of the beam propagates to the MSTAR reference mirror and target retro-reflector, where it is returned back through the Measurement Beamsplitter and coupled into a second single-mode optical fiber that feeds a spectrometer operating at visible wavelengths. The other arm of the white-light interferometer was formed by adding a flat mirror at normal incidence to the second output of the Measurement Beamsplitter. The position of this white-light reference mirror was adjusted to match the path length in the two arms, and the tilt was adjusted to match that of the MSTAR reference mirror.

Once the path lengths to the two reference mirrors were matched, a dispersed fringe pattern was recorded from the spectrometer, without the target retro-reflector in place. This is the 'reference' trace shown in Figs. 5a and 5b. The fringe modulation is a result of the dispersion imbalance in the two arms – the light in one arm makes one more pass through the Measurement Beamsplitter. The white-light beam was then stopped down to illuminate just the central hole in the MSTAR reference mirror, the target retro-reflector was then introduced, and a piezo-electric transducer was used to fine-tune its position until the dispersed fringes in the spectrometer – the 'target' trace – matched the 'reference' trace (Fig.5a). At this point the vertex of the target retro-reflector should be coincident with the plane of the MSTAR reference mirror. The technique is very precise; in Fig. 5a it is straightforward to discriminate an offset of order 0.1 fringes, corresponding to a one-way path offset of ~30 nm. The zero condition is also unambiguous, as illustrated by Fig. 5b, in which the target retro-reflector has been moved by one fringe (300 nm). Although the fringes appear well-registered at the shorter wavelengths, a clear offset is introduced at the long wavelength end of the spectrum. Therefore, this dispersed white-light fringe technique establishes an accurate and unambiguous zero point for our target retro.

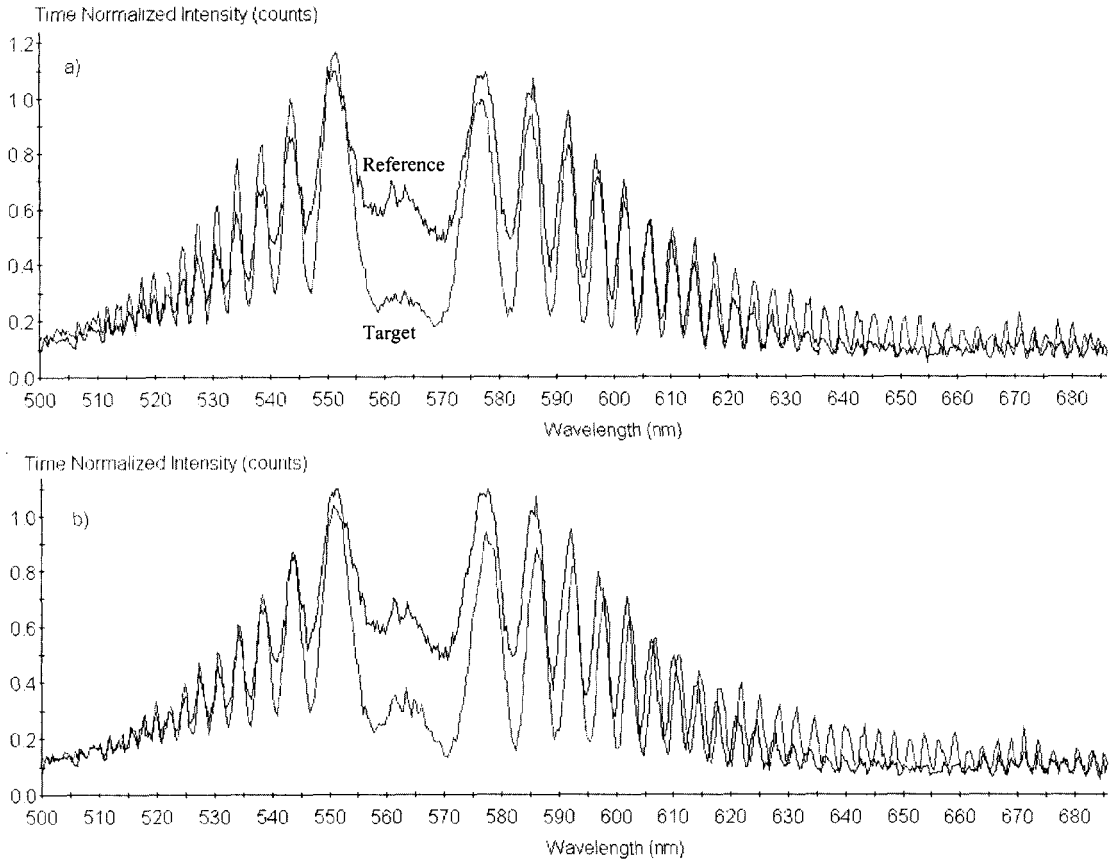

Figure 5: Dispersed white-light fringe patterns used to independently establish the zero point. (a) The zero condition: 'Reference' and 'Target' fringe patterns are fully registered across the spectrum. (b) One fringe off the zero condition: fringe patterns are aligned below 560 nm, but become increasingly offset at longer wavelengths.

With the zero point set, the position of the target retro was measured with MSTAR. The fringe-counting phase-meter was used to take out any thermal or atmospheric drifts during the measurement. After several data points were taken with MSTAR in series, the white-light zero point was re-checked and set as necessary. This process was repeated several times to separate any systematic errors from random errors, and the results are plotted in Fig. 6. From this data, we see the average error of the zero position is less than 0.12 μm, demonstrating that MSTAR has no zero-point offset, to within the uncertainties of the random measurement noise.

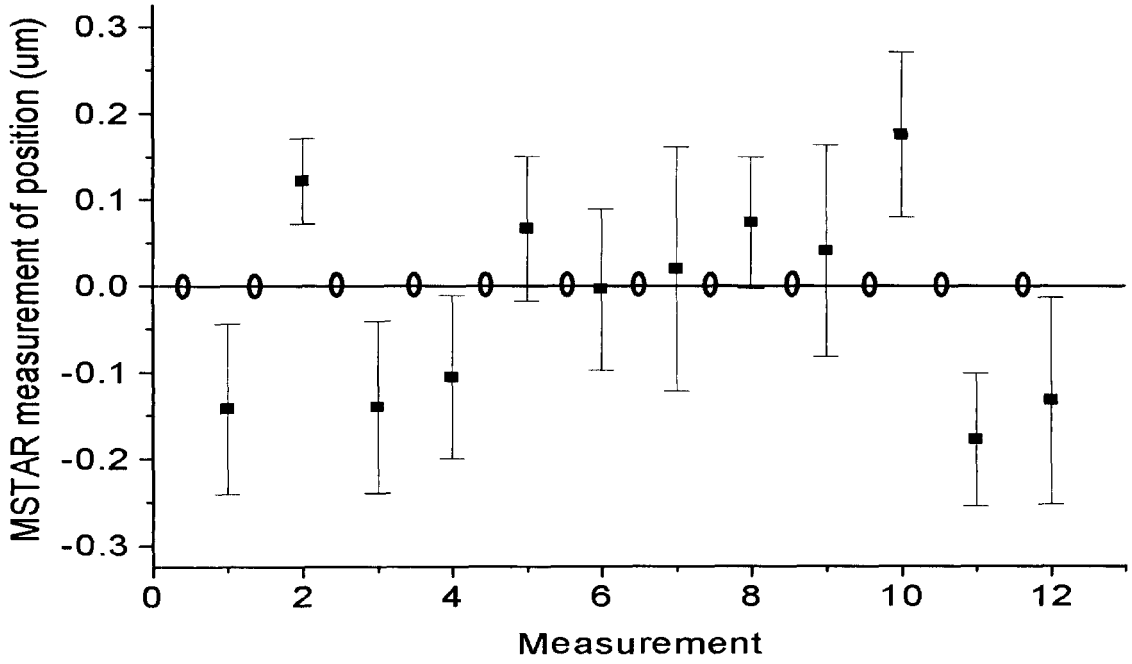

Figure 6: Data from zero-point measurement. Blue circles represent each time the target was set to zero using the dispersed white-light fringe procedure. The squares with error bars represent the MSTAR measurements. The average error of the MSTAR sideband length estimate is less than 0.12 μm, and is consistent with the random measurement noise in the MSTAR readings.

3.4. Zero-out displacement test

The test described in section 3.4 does not rule out the possibility of an anomaly in the MSTAR reading between zero and the start point of the displacement test (~18 cm). Therefore, this final test that we performed was to combine and bridge the gap between the zero-point experiment described in section 3.3, and the displacement test described in section 3.1.

For this test, we began by setting the zero point with the white light interferometer as in section 3.3. Ideally, we would then just move the target out as in the displacement test in section 3.1. However, in order to set the zero point, the quarter waveplate used with the polarizing optics used for isolation of the measurement arm from the reference arm was removed. We could do this at the zero point because the noise sources are common path between the reference mirror and target and cancel. However, as we move the target out, the decreased isolation would decrease the accuracy of the sideband length estimate.

To overcome this, we used the fringe counting phase meter to track the target from the zero point out to a distance where we could insert the polarizing optics. We could then continue to move the target out with the increased isolation as in the earlier displacement test. The increase due to the optical path length through the quarter waveplate was measured as a separate experiment with MSTAR and subtracted off all MSTAR sideband measurement taken after the quarter waveplate was inserted, and the fractional part of the carrier phase was taken off all fringe-counting phasemeter measurements taken after the quarter waveplate was inserted. The results are shown in Fig. 7.

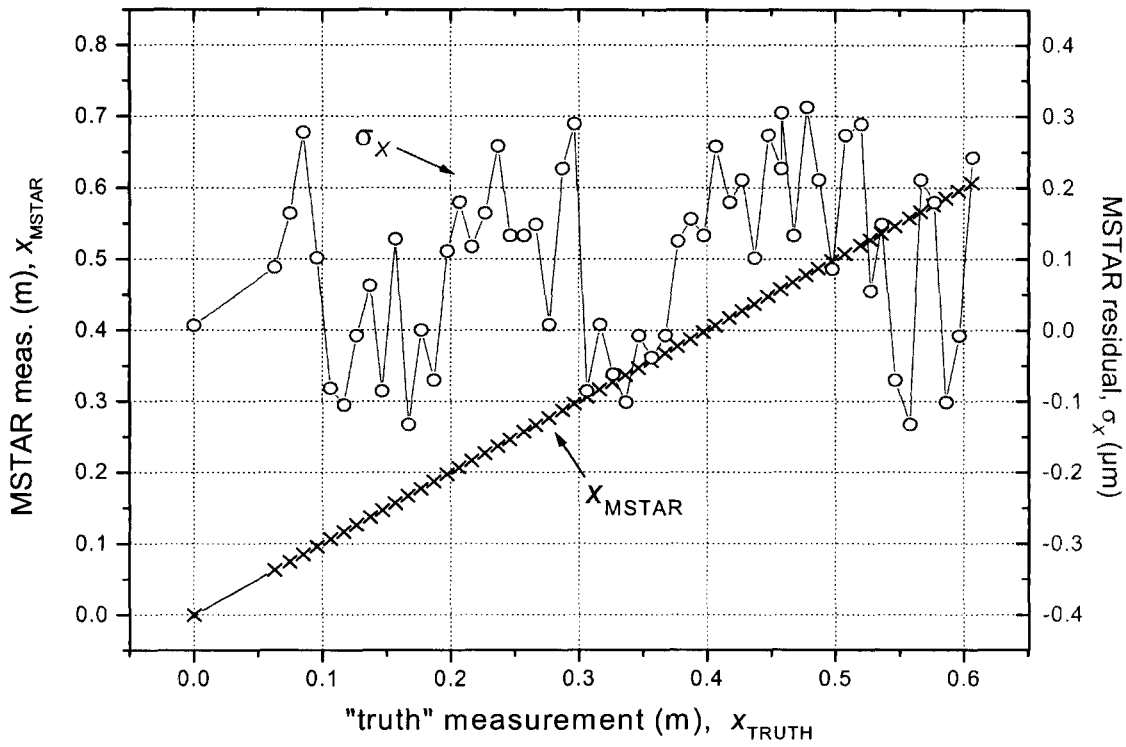

Figure 7: MSTAR measurement vs. truth from zero out to ~0.6 m. The residual error, $\sigma_x = x_{MSTAR} - \Delta x_{TRUTH}$ is overlaid

In this experiment the residual error is computed as $\sigma_x = x_{MSTAR} - \Delta x_{TRUTH}$, since the starting point is zero. The 0.1 um offset of the residual is most likely due to a shift in the target during the insertion of the quarter waveplate. The standard deviation of the residual is 0.13 um and the peak to peak scatter is below the 0.6 um ambiguity of the carrier phase. Therefore we can conclude that there are no anomalies that would give incorrect sideband length estimates between the zero point and other target displacements.

The test described above, along with the stability test described in section 3.2, shows that MSTAR's sideband length estimate measures displacements with accuracy sufficient to resolve the integer-cycle ambiguity, and has no zero-point offset. The tests address only the accuracy of the sideband length estimate (Eq. 2). The MSTAR system simultaneously generates a carrier length estimate (Eq. 1) which, in combination with the sideband length estimate, has subnanometer accuracy. This level of performance was not tested in the experiments.

3.5. Beamsplitter measurements

MSTAR has been used to measure the dimensions of optical components in a practical application. One of the technology testbeds for the Terrestrial Planet Finder mission is designed to demonstrate broadband nulling in an interferometer. A pair of beamsplitters are used in a Mach-Zehnder configuration, and deep nulling requires that the thicknesses of these beamsplitters are matched to within 1 micron.

To measure the thickness with MSTAR, the beamsplitter is simply inserted into the target path, between the reference mirror and the target retro-reflector, and the thickness is given by the difference in the MSTAR readings with and without the beamsplitter in place. To accurately compare two beamsplitters, it is important that they are inserted at the

same tilt angle, and with the same lateral position with respect to the beam (since they have a small wedge angle). The MSTAR output gives the group delay at 1.3 μm; conversion to a mechanical thickness requires knowledge of the dispersion and refractive index of the material. The MSTAR measurements were successful, and consistent with results obtained using a Fourier Transform spectrometer (a more laborious technique).

4. DISCUSSION

4.1. Extension to long-range operation

The MSTAR system has only been demonstrated in the laboratory for stationary targets, at ranges of up to 1 m. Operation at longer range imposes additional requirements on the system performance:

1. The coherence length of the laser source must be larger than the round-trip optical path to the target.
2. The uncertainty in the laser wavelength must be reduced.
3. The uncertainty in the RF modulation frequency must be reduced in order to resolve the integer cycle ambiguity.
4. The system must accommodate the increased photon noise due to the weaker return signal.
5. The weaker target return signal is more prone to leakage and multi-path effects, requiring increased optical isolation.

Each of these items is addressed below.

Coherence length: As noted in section 2.2, the Lightwave NPRO laser has a linewidth of 10 kHz. The associated coherence length of 30 km is therefore sufficient in principle for target distances of up to 15 km.

Laser wavelength uncertainty: Obtaining range accuracy σ_x at range x, requires knowledge of the laser wavelength to a fraction σ_x/x. For example, if x = 100 m and σ_x = 10 nm, then the wavelength must be known with fractional uncertainty less than 10^{-10}. High accuracy measurements over long distances will require a frequency stabilized laser source. Since it is the knowledge of the laser frequency that is important, and not just the frequency stability, commonly used Fabry-Perot cavity references cannot be relied upon, since the cavity is prone to long-term drift. Therefore, we must use an atomic or molecular resonant transition as a frequency reference. The 1.319-μm wavelength NPRO laser currently used for MSTAR has a frequency of 2.3×10^{14} Hz. In order to achieve a position uncertainty of 10 nm over a target separation of 100 m, we must know the laser frequency to within 23 kHz. We have investigated a variety of frequency standards and locking techniques that could achieve this level of frequency accuracy. We believe the best frequency standards for MSTAR would be either molecular iodine or methane. Methane may be used directly with the laser wavelength of 1.319 μm, whereas iodine would require the laser frequency to be doubled to a give a wavelength of 659 nm. Locking a doubled 1319 nm laser to iodine has already been demonstrated[14] with frequency uncertainty of 2.4×10^{-10} (55 kHz). The frequency stabilization system locks on the Lamb-dip[15] at the center of the Doppler broadened absorption profile, using am FM spectroscopy technique similar to that used in common Pound-Drever-Hall[16] locking systems. We believe that similar performance may be achieved using methane without the need for frequency doubling.

Modulation frequency uncertainty: Resolving the integer-cycle ambiguity requires a range resolution of ~100 nm for the sideband length estimate. The phase modulation frequency must therefore be known with fractional uncertainty less than (100 nm / x). For x = 100 m, the knowledge requirement is 10^{-9}, easily met by a number of frequency standards[17]. Compact Rubidium-based systems have an accuracy of $\sim 5 \times 10^{-11}$; laser-cooled Cesium systems approach 10^{-15}.

Increased photon noise: As the photon rate for the return signal is reduced, shot noise becomes the dominant source of random noise in the system. The photon rate can be increased by using a higher power laser, or by increasing the diameter of the target beam and retro-reflector to minimize diffraction losses. This is not necessary, however, since the coherent integration time can be increased arbitrarily, even in the presence of vibration and target motion, using the carrier-aided smoothing technique (section 4.2).

Increased leakage: The weaker return signal is also more susceptible to multi-path effects and leakage from the reference part of the beam. Higher laser power and longer integration times are not going to help with this systematic

error. In the far-field limit, the optical return loss for the target beam is proportional to d^4, where d is the outgoing beam diameter. A large target beam is therefore highly advantageous. The isolation properties of the beam launcher are also likely to be improved by going to a more compact design that minimizes the effects of diffraction, and uses angle-polished fibers to minimize back-reflections.

In summary, we do not believe there are serious obstacles to scaling the performance of MSTAR to ranges of 100 m or more. Of the items listed above, the last one probably warrants the most attention, and will be the subject of further investigation.

4.2. Moving targets

The discussion and analysis up to this point has assumed that the length being measured is constant over the duration of the measurement time. As the range is increased, the returned signal power goes down, and longer coherent integration times are required to resolve the integer cycle ambiguity. The requirement of no motion over this interval then becomes restrictive for many applications; for example, large structures are liable to bend and flex, and optics distributed over multiple spacecraft may exhibit large relative motions.

Fortunately, MSTAR is able to overcome this problem using a technique called 'Carrier-Aided Smoothing', first developed for Global Positioning System applications[18]. The MSTAR sensor generates two estimates of the distance: the carrier length estimate based on the optical phase of the carrier frequency (Eq. 1), and the sideband length estimate based on the phase difference between the sidebands (Eq. 2). The carrier length estimate gives the change in range over the measurement time, relative to the starting value, precise to the nanometer level. This range vs time can then be subtracted off the time series generated by the sideband length estimate. Having removed the effects of motion, we can average the sideband length estimate coherently over an arbitrarily long time interval to increase the signal-to-noise ratio. The result obtained gives the absolute range for the start of measurement time interval, which can be combined with the time series of the carrier length estimate to give an absolute measurement of the range as a function of time.

4.3. Miniaturization

The MSTAR optics are currently implemented as a laboratory breadboard, as shown in Figure 3, and are clearly unsuitable for most practical applications. We do not, however, expect miniaturization to be an issue, because our design is based on the optics developed for the Space Interferometry Mission (SIM). The SIM beam launcher optics has been miniaturized, packaged in prototype models and work is ongoing to build a flight version. A picture of one of the SIM prototypes is shown in Figure 8.

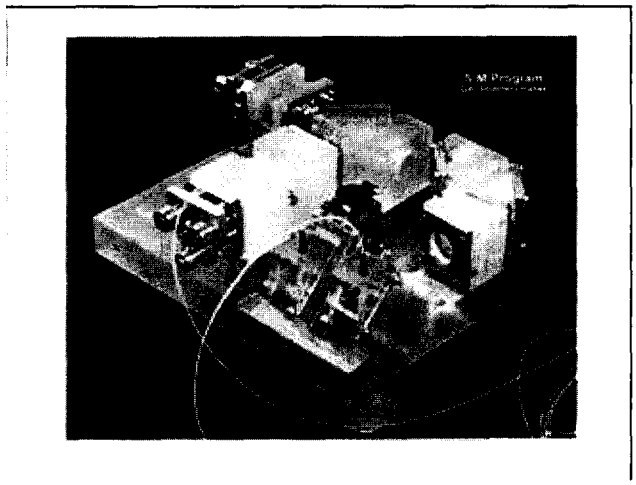

Figure 8: Photograph of a prototype metrology beam launcher developed for the Space Interferometry Mission. The optical isolation performance is similar to that needed for MSTAR. Substantial effort went into producing an athermal design for SIM (note the zerodur base), which would not be needed for MSTAR in most applications. The square base is approximately 6 inches on a side.

5. SUMMARY

We have described the architecture and operation and validation of the MSTAR sensor, a new distance-measuring system based on the use of fast phase modulators. The target modulator generates carrier sidebands – the multiple 'colors' of an absolute metrology system – which are down-converted by the sidebands produced by the local modulator, enabling low-speed detection and signal processing. The beam-launcher is optimized to minimize cross-talk and leakage between the beams, so that we can measure phase differences with an accuracy of 0.3 mrad. The combination of high-speed modulation (40 GHz) and high phase resolution lead to an absolute range resolution of 0.1 um, sufficient to resolve the integer cycle ambiguity of standard laser metrology systems (also an integral part of the MSTAR sensor), and making possible long-range distance measurement with unprecedented accuracy. A dispersed white light interferometry technique was used to independently validate the zero point of the experiment and we have closed the gap in previous experiments between the zero point and displacement tests. Although MSTAR has only been demonstrated over distances of up to 1 m, we show that there are no major obstacles to achieving sub-micron performance over much longer ranges. We believe that such a sensor will become a key part of future interferometer systems.

The work described in this paper was performed at the Jet Propulsion Laboratory, California Institute of Technology, under contract with the National Aeronautics and Space Administration.

REFERENCES

1. N. Bobroff, "Recent advances in displacement measuring interferometry," *Meas. Sci. Technol.*, vol. 4, pp. 907-926, 1993.
2. F. Zhao, "Demonstration of sub-Angstrom cyclic non-linearity using wavefront-division sampling with a common-path laser heterodyne interferometer", American Society of Precision Engineering Annual Meeting, Arlington, VA, Nov 10-15 (2001)
3. O. Bock, "Relative positioning precision of the wide-angle airborne laser ranging system," *J. Opt. A*, vol. 1, pp. 77-82, 1999.
4. I. Fujima, S. Iwasaki, and K. Seta, "High-resolution distance meter using optical intensity modulation at 28 GHz," *Meas. Sci. Technol.*, vol. 9, pp. 1049-1052, 1998.
5. J. M. Payne, D. Parker, and R. G. Bradley, *Rev. Sci. Inst.*, vol. 63, pp. 3311-3316, 1992.
6. R. Dandliker, R. Tharlman, and D. Prongue, "Two-wavelength laser interferometry using super-heterodyne detection," *Opt. Lett.*, vol. 13, pp. 339-343, 1988.
7. J. A. Stone, A. Stejskal, and L. Howard, "Diode lasers in length metrology: application to absolute distance interferometry," *Cal Lab*, 1999.
8. D. Xiaoli and S. Katuo, "High-accuracy absolute distance measurement by means of wavelength scanning heterodyne interferometry," *Meas. Sci. Technol.*, vol. 9, pp. 1031-1035, 1998.
9. P. de Groot, "Three-color laser-diode interferometer," *Appl. Opt.*, vol. 30, pp. 3612-3616, 1991.
10. C. C. Williams and H. K. Wickramasinghe, "Absolute optical ranging with 200-nm resolution," *Opt. Lett.*, vol. 14, pp. 542-544, 1989.
11. X. H. Zhang, M.-C. Oh, A. Szep, W. H. Steier, Z. C, L. R. Dalton, H. Erlig, Y. Chang, D. H. Chang, and H. R. Fetterman, *Appl. Phys. Lett.*, vol. 78, pp. 3136, 2001.
12. R. N. Bracewell, "The Fourier Transform and its applications", McGraw-Hill, New York, 1986.
13. P. Halverson, D. Johnson, A. Kuhnert, S. Shaklan, R. Spero, "A multichannel averaging phasemeter for picometer precision laser metrology" *Proc. SPIE*, **3740**, 646-649 (1999).
14. A. Arie, M. L. Bortz, M. M. Fejer and R. L. Byer, "Iodine spectroscopy and absolute frequency stabilization with the second harmonic of the 1319-nm Nd:YAG laser", *Opt. Lett.*, **18**, 1757-1759, (1993)
15. V. S. Levtokov, "Saturation spectroscopy in high resolution laser spectroscopy," *Topics in Applied Physics*, **16** 849 (1991).
16. R.W.P. Drever, J. L. Hall, F. V. Kowalski, J. Hough, G. M. Ford, A. J. Munley, and H. Ward, "Laser Phase and Frequency Stabilization Using and Optical Resonator", *Appl. Phys. B*, **31**, 97 (1983).
17. National Institute of Standards and Technology website, Time and Frequency division, http://www.boulder.nist.gov/timefreq/
18. R. Hatch, "The Synergism of GPS Code and Carrier Measurements," Proceedings of 3rd International Geodetic Symposium on Satellite Doppler Positioning, DMA/NGS, pp. 1213-1232, Washington, D.C. (1982)